Mathematical Modelling and Numerical Simulation with Applications, 2025, 5(2), 257–279

https://dergipark.org.tr/en/pub/mmnsa
ISSN Online: 2791-8564 / Open Access
https://doi.org/10.53391/mmnsa.1529457

RESEARCH PAPER

Application of a fast Fibonacci wavelet method for the fractional cryosphere model

Mulualem Aychluh [1,*,‡]

[1]Department of Mathematics, Samara University, Samara, Afar, Ethiopia

* Corresponding Author
‡ muleaychluh62@gmail.com (Mulualem Aychluh)

Abstract

This paper presents an efficient numerical approach for approximating the fractional-order cryosphere model using a Caputo-Fabrizio derivative with a non-singular exponential decay kernel. We develop a Fibonacci wavelet-based collocation method to solve the system, transforming the governing equations into nonlinear algebraic equations via operational matrix integration. The resulting system is solved using the Newton-Raphson method. We establish the existence and uniqueness of solutions through the Banach fixed-point theorem and Picard operator theory, and provide a comprehensive convergence analysis of the proposed scheme. Numerical simulations demonstrate the method's effectiveness, with results validated against fourth- and seventh-order fractional Runge-Kutta (RK4 and RK7) methods. The novelty of this work lies in the first application of the Fibonacci wavelet and collocation technique to the cryosphere model, and we represent the model's nonlinear equations using Caputo-Fabrizio fractional derivative. The MATLAB R2016a generated results highlight the method's precision in capturing oscillatory behaviors and sensitivity to fractional order variations $(0 < \wp < 1)$, offering improved climate dynamics modeling through modified memory effect representation.

Keywords: Fibonacci wavelet method; Caputo-Fabrizio fractional derivative; cryosphere model; collocation method

AMS 2020 Classification: 4A08; 65T60; 65M70; 86A08

1 Introduction

Thousands of global issues across various scientific fields such as biology, chemistry, climate science, engineering, accounting and finance, mathematics, and physics have been addressed using mathematical models [1]. The models assist policymakers in making excellent decisions by offering deeper insights and advice. Climate change has emerged as one of the most critical issues of the present time, influencing all aspects of life on Earth [2]. Consequently, climate models are highly important for forecasting the Earth's climate system, allowing specialists to make initial

➤ **Received:** 07.08.2024 ➤ **Revised:** 02.05.2025 ➤ **Accepted:** 13.05.2025 ➤ **Published:** 30.06.2025

future climate scenarios [3]. As a result, formulating and approximating mathematical models have become key tasks for several investigators due to their huge advantages.

Accurately capturing the whole range of dynamical systems, especially those containing memory effects, is one of the primary challenges in mathematical modeling. To overcome this obstacle, researchers have introduced non-integer order operators [4, 5], which offer a promising mathematical approach for enhancing these dynamical models. Because of their numerous applications in physics, mathematics, and climate research, these non-integer order operators have recently attracted a great deal of interest in the scientific community. The main benefit of non-integer-order models is their nonlocal behavior, which makes them more accurate than typical integer-order models in representing physical processes and dynamical systems. The increased accuracy, precision, and realism provided by fractional-order derivative operators have drawn the interest of researchers, highlighting their superiority over conventional integer-order models.

Fractional calculus originated from a historical question about the half-order derivative of functions, which L'Hopital raised to Leibniz three hundred years ago [6]. The Caputo derivative is a popular fractional operator for initial value problems because it maintains the convolution characteristic and works well with integer-order derivatives [6]. However, the Caputo fractional operator has constraints due to its single kernel, which impacts long-term memory properties. Caputo and Fabrizio provided a non-singular fractional derivative with an exponential decay kernel to solve the singularity issue [7]. This operator enhances memory representation, numerical stability, and computational efficiency, making it particularly suitable for climate modeling and long-term cryosphere studies. These features make it superior to traditional Caputo and Riemann-Liouville derivatives, particularly for climate change simulations and long-term cryosphere studies.

In order to find minute changes in the behavior of the Caputo fractional order system, Chakraborty et al. [8] examined how climate change will affect the dynamics of a modified cryosphere model. In [9], Nicolis utilized a pair of dimensionless excess equations to provide a further expression for the dynamics of the cryosphere model:

$$\begin{cases} \dfrac{ds}{dt} = \eta, \\ \dfrac{d\eta}{dt} = \alpha\eta + \beta s - s^3 - s^2\eta + \gamma \sin(\delta t), \end{cases} \tag{1}$$

where $s(t)$ is the extent of the sea ice, which is a crucial indicator of the cryosphere's response to climate variations. $\eta(t)$ is the difference between the mean ocean surface temperature and the sea-ice extent. α is a constant parameter that influences the rate of change of the temperature difference, and β is a coefficient representing the interaction between sea-ice extent and temperature variations. γ representing the effect of seasonal solar forcing. δ represents the frequency of the periodic solar forcing. R denotes the radiative forcing of CO_2, incorporated to analyze the effects of global warming on the cryosphere system. $\wp$ is the fractional order parameter $0 < \wp < 1$, which introduces memory effects and accounts for the non-local behavior of the system.

The effects of radiative forcing were added to the system to evaluate the impacts of global warming in the previous study of the cryosphere model [8]. The (1) was represented using Caputo fractional differential equations with a singular kernel. The model is presented as follows:

$$\begin{cases} {}_0^C D_t^{\wp} s(t) = \eta, \\ {}_0^C D_t^{\wp} \eta(t) = \alpha\eta + \beta s - s^3 - s^2\eta + \gamma \sin(\delta t) + R. \end{cases} \tag{2}$$

The primary objective of this work is to analyze the dynamics of a modified cryosphere model within the framework of an exponential law kernel fractional operator. The fractional derivative has recently gained significant attention among researchers and academics due to its unique properties. Given the remarkable characteristics of the non-singular fractional operator, we investigate a fractional version of the cryosphere model (2). This is accomplished by replacing the singular Caputo time-fractional derivative equations, leading to the formulation of the Caputo-Fabrizio (C-F) model in the following form:

$$\begin{cases} {}_0^{CF}D_t^{\wp} S(t) = \eta, \\ {}_0^{CF}D_t^{\wp} \eta(t) = \alpha\eta + \beta s - s^3 - s^2\eta + \gamma \sin(\delta t) + R. \end{cases} \tag{3}$$

The use of fractional differential operators improves climate modeling by offering a more accurate and realistic representation of complex climate dynamics, particularly those influenced by memory effects and long-range dependencies. Traditional integer-order models assume that a system's behavior depends solely on its current state, whereas fractional-order models incorporate past states, enhancing the precision of climate predictions. The memory effect captured by the Caputo-Fabrizio fractional operator is essential for improving the accuracy of the cryosphere model. It enables the model to better represent historical dependencies, capture oscillatory behavior, reduce numerical errors, and enhance long-term climate forecasts. Consequently, the fractional-order Fibonacci wavelet (FW) approach emerges as a more reliable and efficient method for solving complex cryosphere dynamics compared to traditional integer-order models. The majority of complicated phenomena in nature are nonlinear. Nonlinear equations describe the most significant processes on the planet. Since the equations are often too complicated, both in number and form, to find exact values [10], researchers have extensively studied numerical approximations based on wavelets for solving linear and nonlinear fractional differential equations [11]. Since wavelet-based techniques are effective at approximating both linear and nonlinear differential equations, including those with fractional orders, they have attracted a lot of attention in the scientific and engineering categories in recent years. Wavelets are a well-liked option for solving differential equations because of their high accuracy and efficiency in processing. Numerous authors in the literature have employed a variety of wavelet functions, including Bernoulli [12], Laguerre [13], Chebyshev [14], Jacobbi [15], Gegenbauer [16], modified Laguerre [17], and Legendre [18] wavelets. Some interesting methods are using Laguerre wavelets to solve nonlinear differential equations with variable delay [19] and the ultraspherical wavelets collocation method to solve the Benjamin-Bona-Mahony equation [20]. Fibonacci wavelets are derived from Fibonacci polynomials $F_n(t)$ and have several benefits in comparison to the other wavelet techniques.

- $F_n(t)$ contains fewer terms compared to other wavelet-based methods such as Gegenbauer polynomials $G_n(t)$, Legendre polynomials $L_n(t)$ and Laguerre polynomials $J_n(t)$, making them computationally efficient. For instance, $F_{10}(t)$ consists of six terms, while $J_{10}(t)$ has ten, with this difference increasing as n increases.
- The Fibonacci wavelet method maintains high accuracy while being computationally faster than traditional wavelet approaches.
- Fibonacci wavelets are not based on orthogonal polynomials. The Fibonacci polynomials can be represented in terms of other orthogonal polynomials.

$$F_m(x) = s^2 U_m\left(\frac{x}{2s}\right), \quad m \geq 0,$$

where $U_m(x)$ is the second type Chebyshev polynomial [21] and $s^2 = -1$.

Researchers have successfully applied the FW schemes to approximate various nonlinear differential equations, including Stratonovich-Volterra integral equations [22], delay problems [23], and optimal control problems [24]. Srivastava, Shah, and Nayied in [25] utilized the Fibonacci Wavelet technique to approximate the nonlinear Hunter-Saxton equation, while others applied the method to time-fractional telegraph equations with boundary conditions [26]. Further applications of the FW approach include the design of fast FW procedures to approximate the mathematical model of HIV-infected CD4+ T cells [27], and the solution of time-varying delay equations [23]. Motivated by these advancements, the current study applies a fast Fibonacci wavelet based collocation scheme incorporating the non-singular C-F fractional derivative operator to the recently modified dynamics of the cryosphere model.

This work improves the modified surface energy balance-mass balance cryosphere model already investigated by Chakraborty et al. [8]. The original model was described using Caputo fractional differential equations, but the present study replaces the singular Caputo derivative with the Caputo-Fabrizio fractional operator with a non-singular exponential decay kernel. The authors of [8] pointed out that limited research has been done on the model (1) and they focused on its modification and solution. They used the fractional seventh-order Runge-Kutta method (RK7) to approximate their modified model. The present study aims to investigate the application of the Fibonacci wavelet-based collocation method in climate system modeling. The originality of this work lies in the application of the Fibonacci wavelet technique to approximate the cryosphere model. To the best of our knowledge, this is the first study to apply the fast Fibonacci wavelet method to approximate the cryosphere model.

The use of fractional differential operators in climate modeling leads to better representation of memory effects, more accurate simulation of climate change, enhanced modeling of nonlinear and chaotic dynamics, and improved computational efficiency [28]. The motivation for this study comes from the need for a more accurate and efficient numerical scheme to approximate the climate system. The effectiveness of Fibonacci wavelet-based collocation technique has been investigated in various mathematical equations, demonstrating their potential in solving differential and integral equations with high accuracy [29]. However, their application to climate systems has not been extensively explored. Given the complexity and chaotic nature of climate models, advanced numerical techniques such as wavelet-based approaches could provide improved stability and computational efficiency. This study aims to bridge this gap by evaluating the performance of Fibonacci wavelet-based collocation method in climate system modeling.

This study does not propose modifications to the cryosphere model's structure itself, which is one of the limitations of the paper. Instead, it focuses on approximating the system using the Fibonacci wavelet collocation method. Consequently, the findings depend on the accuracy of the numerical scheme, rather than introducing new dynamics into the model. The study relies on numerical approximations of the system through the Fibonacci wavelet collocation method. Furthermore, small variations in model parameters can lead to significantly different outcomes, which can limit its predictive power and generalizability. The accuracy and convergence of the solution can be highly sensitive to the choice of parameters in the cryosphere model. Future work could address these limitations by incorporating adaptive numerical techniques or testing the model against real climate data, ensuring its robustness across different climate scenarios.

The study contributes to the climate field by providing an effective numerical scheme for the dynamics of the mass balance-surface energy balance model of the cryosphere. This study is important because it applies the fast Fibonacci wavelet approach to approximate the fractional cryosphere model via the Caputo-Fabrizio fractional derivative, which has a non-singular ex-

ponential decay kernel. The cryosphere model plays a crucial role in understanding climate change dynamics, and incorporating fractional derivatives enhances the model's ability to capture memory effects and nonlinear behavior more accurately than traditional integer-order models. This paper provides a more efficient and accurate method for solving fractional-order cryosphere model. The introduction of Fibonacci wavelets and the Caputo-Fabrizio fractional operator distinguishes it from previous studies, making it a novel and valuable contribution to the cryosphere model.

In the present section, some introductions of the mathematical modelling, fractional cryosphere model, Fibonacci wavelet, and background of fractional operators are written. The following is an outline of this paper: Section 2 presents the definitions of the C-F fractional calculus. We define the properties of the FWs and the approximation of a function using the FW basis. We also discuss the existence and uniqueness of the solution and provide a convergence analysis of the proposed FW and collocation points. Numerical approximations based on FWs for the fractional cryosphere model are presented in Section 3. Results and discussion are found in Section 4. The paper ends in Section 5.

2 Fundamental concepts

This section reviews the Caputo-Fabrizio fractional calculus, Fibonacci polynomials, and Fibonacci wavelets that will be applied throughout this study.

Caputo-Fabrizio fractional calculus

Caputo and Fabrizio [7] initially defined the fractional derivative and the associated integral with a non-singular exponential kernel, addressing significant weaknesses in previous definitions of fractional calculus. Key details and fundamental properties of this operator are outlined below.

Definition 1 *For $\wp \in (0,\ 1)$, and $\phi(t) \in H^1(\alpha,\ \beta)$, the C-F fractional derivative [7, 30] is defined as:*

$$^{CF}D_t^{\wp}\phi(t) = \frac{\Phi(\wp)}{1-\wp}\int_0^t \phi'(x)\exp\left(\varsigma(t-x)\right)dx,$$

where $\Phi(\wp) = 1-\wp+\dfrac{\wp}{\Gamma(\wp)}$ *and* $\varsigma = -\dfrac{\wp}{1-\wp}$.

Definition 2 *For $\wp \in (0,\ 1)$, and $\phi(t) \in H^1(\alpha,\ \beta)$, the C-F fractional derivative, as modified by Losada and Nieto, is defined as [31]:*

$$^{CF}D_t^{\wp}\phi(t) = \frac{(2-\wp)\Phi(\wp)}{2(1-\wp)}\int_0^t \phi'(x)\exp\left(\varsigma(t-x)\right)dx. \tag{4}$$

The integral corresponding to the derivative in (4) was updated by Losada and Nieto [31] as follows.

Definition 3 *For $0 < \wp < 1$, the C-F integral of fractional order $\wp$ of a function $\phi(t)$ is given by [31]:*

$$^{CF}I_t^{\wp}\phi(t) = \frac{2(1-\wp)}{(2-\wp)\Phi(\wp)}\phi(t) + \frac{2\wp}{(2-\wp)\Phi(\wp)}\int_0^t \phi(x)\,dx. \tag{5}$$

The Fibonacci polynomials and wavelets

For all $t \in \mathbb{R}^+$, the Fibonacci polynomials are generated by the recurrence relation:

$$F_n(t) = tF_{n-1}(t) + F_{n-2}(t), \quad \forall n \geq 2,$$

with starting polynomials $F_0(t) = 1, \ F_1(t) = t$. Furthermore, the polynomial expansion of the Fibonacci polynomials can also be expressed as [22]

$$F_n(t) = \sum_{m=0}^{\lfloor n/2 \rfloor} \binom{n-m}{m} t^{n-2m}, \quad \forall n \geq 0.$$

The Fibonacci wavelets on the interval $[0, \ 1]$ are defined as [25, 26]:

$$\lambda_{s,\,n}(t) = \begin{cases} \dfrac{2^{(d-1)/2}}{\sqrt{\psi_n}} F_n\left(2^{d-1}t - s + 1\right), & \dfrac{s-1}{2^{d-1}} \leq t < \dfrac{s}{2^{d-1}}, \\ 0, & \text{otherwise}, \end{cases}$$

where $F_n(t)$ is n^{th} degree Fibonacci polynomials, $d \in \mathbb{N}$ denote the maximum level of resolution, $s = 1, \ 2, \ 3, \ \ldots, 2^{d-1}$ denote the translation parameter, and $1/\sqrt{\psi_n}$ is a normalization factor and can be computed as remove:

$$\psi_n = \int_0^1 \left(F_n(t)\right)^2 dt, \quad (n = 0, \ 1, \ \ldots, \ N-1).$$

When the translation parameter α and dilation parameter $\wp$ vary continuously, the following family of continuous wavelets is obtained:

$$\lambda_{\alpha,\,\wp}(t) = |\alpha|^{-1/2} \lambda\left(\frac{t-\wp}{\alpha}\right), \ \alpha, \ \wp \in \mathbb{R}, \ \alpha \neq 0.$$

If we choose $\alpha = \alpha_0^{-d}$ and $\wp = n\alpha_0^{-d}\wp_0$, $\alpha_0 > 1, \ \wp_0 > 1$, and $n, \ d \in \mathbb{Z}^+$ and the discrete wavelet family is introduced as:

$$\lambda_{d,\,n}(t) = |\alpha_0|^{d/2} \lambda\left(\alpha_0^d t - n\wp_0\right),$$

where $\lambda_{d,\,n}(t)$ is the wavelet basis in $L^2(\mathbb{R})$.

Operational integration matrix

In particular, if $d = 1$ and $N = 10$, then the ten basis of FW functions are computed as:

$$\begin{aligned} \lambda_{1,0}(t) &= 1, \ \lambda_{1,1}(t) = \sqrt{3}t, \ \lambda_{1,2}(t) = \frac{1}{2}\sqrt{\frac{15}{7}}(t^2+1), \ \lambda_{1,3}(t) = \sqrt{\frac{105}{239}}(t^3+2t), \\ \lambda_{1,4}(t) &= 3\sqrt{\frac{35}{1943}}(t^4+3t^2+1), \ \lambda_{1,5}(t) = \frac{3}{4}\sqrt{\frac{385}{2582}}(t^5+4t^3+3t), \end{aligned}$$

$$
\begin{aligned}
\lambda_{1,6}(t) &= 3\sqrt{\frac{5005}{1268209}}(t^6+5t^4+6t^2+1),\\
\lambda_{1,7}(t) &= 3\sqrt{\frac{5005}{2827883}}(t^7+6t^5+10t^3+4t),\\
\lambda_{1,8}(t) &= \frac{3}{2}\sqrt{\frac{85085}{28195421}}(t^8+7t^6+15t^4+10t^2+1),\\
\lambda_{1,9}(t) &= 3\sqrt{\frac{1616615}{5016284989}}(t^9+8t^7+21t^5+20t^3+5t),\\
\lambda_{1,10}(t) &= 3\sqrt{\frac{1616615}{119941544471}}(t^{10}+9t^8+28t^6+35t^4+15t^2+1) \qquad (6)
\end{aligned}
$$

where

$$\lambda_{10}(t) = [\lambda_{1,0}(t),\ \lambda_{1,1}(t),\ \lambda_{1,2}(t),\ \ldots,\ \lambda_{1,9}(t)]^T.$$

Integration of each element of the above vector with respect to x, from 0 to t, and expressing them as a linear combination of the wavelet basis, we obtain:

$$\int_0^t \lambda_{1,0}(x)\,dx = \left[0\ \frac{1}{\sqrt{3}}\ 0\ 0\ 0\ 0\ 0\ 0\ 0\right]\lambda_{10}(t),$$

$$\int_0^t \lambda_{1,1}(x)\,dx = \left[-\frac{\sqrt{3}}{2}\ 0\ \sqrt{\frac{7}{5}}\ 0\ 0\ 0\ 0\ 0\ 0\right]\lambda_{10}(t),$$

$$\int_0^t \lambda_{1,2}(x)\,dx = \left[0\ \frac{\sqrt{5}}{6\sqrt{7}}\ 0\ \frac{\sqrt{239}}{42}\ 0\ 0\ 0\ 0\ 0\right]\lambda_{10}(t),$$

$$\int_0^t \lambda_{1,3}(x)\,dx = \left[-\frac{\sqrt{105}}{2\sqrt{239}}\ 0\ \frac{7}{2\sqrt{239}}\ 0\ \frac{\sqrt{1943}}{4\sqrt{717}}\ 0\ 0\ 0\ 0\ 0\right]\lambda_{10}(t),$$

$$\int_0^t \lambda_{1,4}(x)\,dx = \left[0\ 0\ 0\ \frac{\sqrt{717}}{5\sqrt{1943}}\ 0\ \frac{4\sqrt{2582}}{5\sqrt{21373}}\ 0\ 0\ 0\ 0\right]\lambda_{10}(t),$$

$$\int_0^t \lambda_{1,5}(x)\,dx = \left[\frac{-\sqrt{385}}{4\sqrt{2582}}\ 0\ 0\ 0\ \frac{\sqrt{21373}}{24\sqrt{2582}}\ 0\ \frac{\sqrt{1268209}}{24\sqrt{33566}}\ 0\ 0\ 0\right]\lambda_{10}(t),$$

$$\int_0^t \lambda_{1,6}(x)\,dx = \left[0\ 0\ 0\ 0\ 0\ \frac{4\sqrt{33566}}{7\sqrt{1268209}}\ 0\ \frac{\sqrt{2827883}}{7\sqrt{1268209}}\ 0\ 0\right]\lambda_{10}(t),$$

$$\int_0^t \lambda_{1,7}(x)\,dx = \left[-\frac{3\sqrt{5005}}{4\sqrt{2827883}}\ 0\ 0\ 0\ 0\ 0\ \frac{\sqrt{1268209}}{8\sqrt{2827883}}\ 0\ \frac{\sqrt{28195421}}{4\sqrt{48074011}}\ 0\right]\lambda_{10}(t),$$

$$\int_0^t \lambda_{1,8}(x)\,dx = \left[0\ 0\ 0\ 0\ 0\ 0\ 0\ \frac{\sqrt{48074011}}{18\sqrt{28195421}}\ 0\ \frac{\sqrt{5016284989}}{18\sqrt{535712999}}\right]\lambda_{10}(t),$$

$$\int_0^t \lambda_{1,\,9}\,(x)\,dx = \left[-3\sqrt{\frac{323323}{25081424945}}\;\; 0\;\; 0\;\; 0\;\; 0\;\; 0\;\; 0\;\; \frac{\sqrt{535712999}}{5\sqrt{5016284989}}\;\; 0\right]\lambda_{10}\,(t)\,.$$

Hence,

$$\int_0^t \lambda\,(x)\,dx = A_{10\times 10}\lambda_{10}\,(t) + B_{10\times 1}\,(t)\,, \tag{7}$$

where

$$A_{10\times 10} = \begin{bmatrix}
0 & \frac{1}{\sqrt{3}} & 0 & 0 & 0 & 0 & 0 & 0 & 0 & 0 \\
-\frac{\sqrt{3}}{2} & 0 & \sqrt{\frac{7}{5}} & 0 & 0 & 0 & 0 & 0 & 0 & 0 \\
0 & \frac{\sqrt{5}}{6\sqrt{7}} & 0 & \frac{\sqrt{239}}{42} & 0 & 0 & 0 & 0 & 0 & 0 \\
-\frac{\sqrt{105}}{2\sqrt{239}} & 0 & \frac{7}{2\sqrt{239}} & 0 & \frac{\sqrt{1943}}{4\sqrt{717}} & 0 & 0 & 0 & 0 & 0 \\
0 & 0 & 0 & \frac{\sqrt{717}}{5\sqrt{1943}} & 0 & \frac{4\sqrt{2582}}{5\sqrt{21373}} & 0 & 0 & 0 & 0 \\
-\frac{\sqrt{385}}{4\sqrt{2582}} & 0 & 0 & 0 & \frac{\sqrt{21373}}{24\sqrt{2582}} & 0 & \frac{\sqrt{1268209}}{24\sqrt{33566}} & 0 & 0 & 0 \\
0 & 0 & 0 & 0 & 0 & \frac{4\sqrt{33566}}{7\sqrt{1268209}} & 0 & \frac{\sqrt{2827883}}{7\sqrt{1268209}} & 0 & 0 \\
-\frac{3\sqrt{5005}}{4\sqrt{2827883}} & 0 & 0 & 0 & 0 & 0 & \frac{\sqrt{1268209}}{8\sqrt{2827883}} & 0 & \frac{\sqrt{28195421}}{4\sqrt{48074011}} & 0 \\
0 & 0 & 0 & 0 & 0 & 0 & 0 & \frac{\sqrt{48074011}}{18\sqrt{28195421}} & 0 & \frac{\sqrt{5016284989}}{18\sqrt{535712999}} \\
-3\sqrt{\frac{323323}{25081424945}} & 0 & 0 & 0 & 0 & 0 & 0 & 0 & \frac{\sqrt{535712999}}{5\sqrt{5016284989}} & 0
\end{bmatrix},$$

and

$$B_{10\times 1}\,(t) = \left[0\;\; 0\;\; 0\;\; 0\;\; 0\;\; 0\;\; 0\;\; 0\;\; 0\;\; \frac{\sqrt{11941544471}}{10\sqrt{5016284989}}\lambda_{1,\,10}\,(t)\right]^T.$$

Existence and uniqueness of the result

A crucial aspect of mathematical analysis that ensures well-defined results, clear calculations, and facilitates future computations is showing the existence and uniqueness of the results. With the help of the Banach fixed-point theorem and Picard operator, we need to show that the result of (3) exists and is one.

Theorem 1 *In the region* $[0,\ \mathscr{T}] \times \mathscr{R}$, *where*

$$\mathscr{R} = \left\{(s,\ \eta) \in \mathbb{R}^2 :\ \|s\| < \rho_1,\ \|\eta\| < \rho_2\right\},$$

and $\mathscr{T} < +\infty$, *the result of* (3) *exists and is one.*

Proof Let $S\,(t) = (s\,(t)\,,\ \eta\,(t))$ and $S_1\,(t) = (s_1\,(t)\,,\ \eta_1\,(t))$ and $C\,(t,\ S) = (C_1\,(t,\ S)\,,\ C_2\,(t,\ S))$, where

$$\begin{cases} C_1\,(t,\ S) = \eta, \\ C_2\,(t,\ S) = \alpha\eta + \beta s - s^3 - s^2\eta + \gamma\sin\,(\delta t) + R. \end{cases}$$

C is defined on $[0,\ \mathscr{T}]\times\mathscr{R}$. Let $K=\sup_{\mathscr{R}}\|C\left(t,\ S\right)\|$ and consider the norm as $\|S\left(t\right)\|=\sup_{t\in[0,\ \mathscr{T}]}|S\left(t\right)|$. We show that there is some parameter φ such that:

$$\|C\left(t,\ S\right)-C\left(t,\ S_1\right)\|\leq\varphi\|S-S_1\|.$$

Thus,

$$\|C\left(t,\ S\right)-C\left(t,\ S_1\right)\|=\|\eta-\eta_1+\alpha\left(\eta-\eta_1\right)+\beta\left(s-s_1\right)+s_1^3-s^3+s_1^2\eta_1-s^2\eta\|.$$

Applying the triangular inequality, we have

$$\begin{aligned}
&\leq \|\eta-\eta_1\|+\alpha\|\eta-\eta_1\|+\beta\|s-s_1\|+\|s^3-s_1^3\|+\|s^2\eta-s_1^2\eta_1\|\\
&\leq (\beta+3\rho_1^2+2\rho_1\rho_2 t)\|s-s_1\|+\left(1+\alpha+\rho_1^2\right)\|\eta-\eta_1\| \qquad (8)\\
&= \varphi_1\|s-s_1\|+\varphi_2\|\eta-\eta_1\|,
\end{aligned}$$

where $\varphi_1=\beta+3\rho_1^2+2\rho_1\rho_2,\ \ \varphi_2=1+\alpha+\rho_1^2$. Let $\varphi=\max\{\varphi_1,\ \varphi_2\}$. Therefore, we have

$$\|C\left(t,\ S\right)-C\left(t,\ S_1\right)\|\leq\varphi\|S-S_1\|.$$

Using the fractional C-F integral, we construct Picard's operator as below:

$$\Delta S=S\left(0\right)+{}^{CF}I_t^{\wp}C\left(t,\ S\right),\quad \wp\in(0,\ 1). \qquad (9)$$

Let

$$\|S-S\left(0\right)\|\leq\lambda.$$

Putting norm on the leftt and right sides of (9), we get:

$$\begin{aligned}
\|\Delta S-S(0)\| &= \|C(t,S)\|{}^{CF}I_t^{\wp}(1)\\
&\leq K\left(\frac{2(1-\wp)}{(2-\wp)\Phi(\wp)}+\frac{2\wp}{(2-\wp)\Phi(\wp)}t\right)<\lambda \qquad (10)
\end{aligned}$$

where the last inequality holds if $\dfrac{2\left(1-\wp\right)}{\left(2-\wp\right)\Phi\left(\wp\right)}+\dfrac{2\wp}{\left(2-\wp\right)\Phi\left(\wp\right)}t<\dfrac{\lambda}{K}$. We now extract a need for the operator Δ to turn into a contraction map. To do so, we begin with:

$$\begin{aligned}
\|\Delta S-\Delta S_1\| &\leq {}^{CF}I_t^{\wp}\left(C\left(t,\ S\right)-C\left(t,\ S_1\right)\right)\leq{}^{CF}\ I_t^{\wp}\|C\left(t,\ S\right)-C\left(t,\ S_1\right)\|\\
&\leq \|C\left(t,\ S\right)-C\left(t,\ S_1\right)\|{}^{CF}I_t^{\wp}\left(1\right) \qquad (11)\\
&\leq \left(\frac{2\left(1-\wp\right)}{\left(2-\wp\right)\Phi\left(\wp\right)}+\frac{2\wp}{\left(2-\wp\right)\Phi\left(\wp\right)}t\right)\varphi\|S-S_1\|.
\end{aligned}$$

From inequality (11), we conclude that Δ is a contraction if

$$\frac{2\left(1-\wp\right)}{\left(2-\wp\right)\Phi\left(\wp\right)}+\frac{2\wp}{\left(2-\wp\right)\Phi\left(\wp\right)}t\leq\frac{1}{\varphi}.$$

We derive a criterion for the operator Δ to be a contraction, thereby applying the Banach Fixed-Point Theorem to conclude that the system (3) has a unique solution when

$$\frac{2\left(1-\wp\right)}{\left(2-\wp\right)\Phi\left(\wp\right)}+\frac{2\wp}{\left(2-\wp\right)\Phi\left(\wp\right)}t\leq\min\left\{\frac{\lambda}{K},\ \frac{1}{\varphi}\right\}.$$

3 Numerical approximation based on Fibonacci wavelets

The method for approximating the solution of the Caputo-Fabrizio fractional cryosphere system using Fibonacci wavelets is shown in this section. Assume that

$$\begin{cases} {}^{CF}D_t^{\wp}s\left(t\right)=P^T\lambda\left(t\right), \\ {}^{CF}D_t^{\wp}\eta\left(t\right)=Q^T\lambda\left(t\right), \end{cases} \tag{12}$$

where

$$P^T=\left[p_{1,\,0},\ \cdots\ p_{1,\,N-1},\ p_{2,\,0},\ \cdots\ p_{2,\,N-1},\ p_{2^{d-1},\,0},\ \cdots\ p_{2^{d-1},\,N-1}\right],$$

$$Q^T=\left[q_{1,\,0},\ \cdots\ q_{1,\,N-1},\ q_{2,\,0},\ \cdots\ q_{2,\,N-1},\ q_{2^{d-1},\,0},\ \cdots\ q_{2^{d-1},\,N-1}\right],$$

$$\text{and}\ \ \lambda\left(t\right)=\left[\lambda_{1,\,0}\left(t\right),\ \ldots,\ \lambda_{1,\,N-1}\left(t\right),\ \lambda_{2,\,0}\left(t\right),\ \ldots,\ \lambda_{2,\,N-1}\left(t\right),\ \lambda_{2^{d-1},\,0}\left(t\right),\ \ldots,\ \lambda_{2^{d-1},\,N-1}\left(t\right)\right].$$

Applying the Caputo-Fabrizio fractional integral to Eq. (12) and using the fundamental theorem of fractional calculus, we obtain:

$$\begin{cases} S\left(t\right)=S\left(0\right)+{}^{CF}I_t^{\wp}\left[P^T\lambda\left(t\right)\right], \\ \eta\left(t\right)=\eta\left(0\right)+{}^{CF}I_t^{\wp}\left[Q^T\lambda\left(t\right)\right]. \end{cases}$$

Using Definition 3, we have:

$$S\left(t\right)=S\left(0\right)+\frac{2\left(1-\wp\right)}{\left(2-\wp\right)\Phi\left(\wp\right)}P^T\lambda\left(t\right)+\frac{2\wp}{\left(2-\wp\right)\Phi\left(\wp\right)}\int_0^t P^T\lambda\left(x\right)dx,$$

$$\eta\left(t\right)=\eta\left(0\right)+\frac{2\left(1-\wp\right)}{\left(2-\wp\right)\Phi\left(\wp\right)}Q^T\lambda\left(t\right)+\frac{2\wp}{\left(2-\wp\right)\Phi\left(\wp\right)}\int_0^t Q^T\lambda\left(x\right)dx.$$

Similarly, use $\lambda\left(t\right)$ to represent the starting values as functions of the known vectors U and V. Therefore, using Eq. (7) to obtain:

$$\begin{cases} S\left(t\right)=U^T\lambda\left(t\right)+\frac{2\left(1-\wp\right)}{\left(2-\wp\right)\Phi\left(\wp\right)}P^T\lambda\left(t\right)+\frac{2\wp}{\left(2-\wp\right)\Phi\left(\wp\right)}P^T\left[A\lambda\left(t\right)+B\left(t\right)\right], \\ \eta\left(t\right)=V^T\lambda\left(t\right)+\frac{2\left(1-\wp\right)}{\left(2-\wp\right)\Phi\left(\wp\right)}Q^T\lambda\left(t\right)+\frac{2\wp}{\left(2-\wp\right)\Phi\left(\wp\right)}Q^T\left[A\lambda\left(t\right)+B\left(t\right)\right]. \end{cases} \tag{13}$$

Now substitute Eq. (13) into Eq. (3), we get:

$$\begin{cases} P^T\lambda(t) = V^T\lambda(t) + \dfrac{2(1-\wp)}{(2-\wp)\Phi(\wp)}Q^T\lambda(t) + \dfrac{2\wp}{(2-\wp)\Phi(\wp)}Q^T[A\lambda(t)+B(t)], \\ Q^T\lambda(t) = \alpha\left(V^T\lambda(t) + \dfrac{2(1-\wp)}{(2-\wp)\Phi(\wp)}Q^T\lambda(t) + \dfrac{2\wp}{(2-\wp)\Phi(\wp)}Q^T[A\lambda(t)+B(t)]\right) \\ +\beta\left(U^T\lambda(t) + \dfrac{2(1-\wp)}{(2-\wp)\Phi(\wp)}P^T\lambda(t) + \dfrac{2\wp}{(2-\wp)\Phi(\wp)}P^T[A\lambda(t)+B(t)]\right) \\ -\left(U^T\lambda(t) + \dfrac{2(1-\wp)}{(2-\wp)\Phi(\wp)}P^T\lambda(t) + \dfrac{2\wp}{(2-\wp)\Phi(\wp)}P^T[A\lambda(t)+B(t)]\right)^3 \\ -\left(U^T\lambda(t) + \dfrac{2(1-\wp)}{(2-\wp)\Phi(\wp)}P^T\lambda(t) + \dfrac{2\wp}{(2-\wp)\Phi(\wp)}P^T[A\lambda(t)+B(t)]\right)^2 \\ \times\left(V^T\lambda(t) + \dfrac{2(1-\wp)}{(2-\wp)\Phi(\wp)}Q^T\lambda(t) + \dfrac{2\wp}{(2-\wp)\Phi(\wp)}Q^T[A\lambda(t)+B(t)]\right) + \gamma\sin(\delta t) + R. \end{cases} \tag{14}$$

Hence using the collocation points $t_i = \dfrac{2i-1}{2^d N}$, $i = 1, 2, \ldots, 2^{d-1}N$ collocating each equation in (14) to get a system of $2^d N$ number of nonlinear algebraic equations.

$$\begin{cases} P^T\lambda(t_i) = V^T\lambda(t_i) + \dfrac{2(1-\wp)}{(2-\wp)\Phi(\wp)}Q^T\lambda(t_i) + \dfrac{2\wp}{(2-\wp)\Phi(\wp)}Q^T[A\lambda(t_i)+B(t_i)], \\ Q^T\lambda(t_i) = \alpha\left(V^T\lambda(t_i) + \dfrac{2(1-\wp)}{(2-\wp)\Phi(\wp)}Q^T\lambda(t_i) + \dfrac{2\wp}{(2-\wp)\Phi(\wp)}Q^T[A\lambda(t_i)+B(t_i)]\right) \\ +\beta\left(U^T\lambda(t_i) + \dfrac{2(1-\wp)}{(2-\wp)\Phi(\wp)}P^T\lambda(t_i) + \dfrac{2\wp}{(2-\wp)\Phi(\wp)}P^T[A\lambda(t_i)+B(t_i)]\right) \\ -\left(U^T\lambda(t_i) + \dfrac{2(1-\wp)}{(2-\wp)\Phi(\wp)}P^T\lambda(t_i) + \dfrac{2\wp}{(2-\wp)\Phi(\wp)}P^T[A\lambda(t_i)+B(t_i)]\right)^3 \\ -\left(U^T\lambda(t_i) + \dfrac{2(1-\wp)}{(2-\wp)\Phi(\wp)}P^T\lambda(t_i) + \dfrac{2\wp}{(2-\wp)\Phi(\wp)}P^T[A\lambda(t_i)+B(t_i)]\right)^2 \\ \times\left(V^T\lambda(t_i) + \dfrac{2(1-\wp)}{(2-\wp)\Phi(\wp)}Q^T\lambda(t_i) + \dfrac{2\wp}{(2-\wp)\Phi(\wp)}Q^T[A\lambda(t_i)+B(t_i)]\right) + \gamma\sin(\delta t_i) + R. \end{cases}$$

The Newton-Raphson approach for nonlinear systems can be used to approximate the system of $2^d N$ algebraic equations. Lastly, the Fibonacci wavelet solution for the C-F fractional cryosphere model may be obtained by replacing these values of the Fibonacci wavelet coefficients into (13).

Convergence of Fibonacci wavelets

Theorem 2 *Let H be a Hilbert space and W be a closed, finite-dimensional subspace H such that* $\dim W < \infty$ *and $\{u_1, u_2, \ldots, u_n\}$ is any basis for W. Let k be an arbitrary element in H and k_0 be the unique best*

approximation to k out of W. Then [32]

$$\|k - k_0\|_2 = \bar{F}_k,$$

where $\bar{F}_k = \sqrt{\dfrac{\hat{M}(k,\ u_1,\ u_2,\ \ldots,\ u_n)}{\hat{M}(u_1,\ u_2,\ \ldots,\ u_n)}}$ *and* $\hat{M}$ *is introduced as follows [32]:*

$$\hat{M}(k,\ u_1,\ u_2,\ \ldots,\ u_n) = \begin{vmatrix} \langle k,\ k\rangle & \langle k,\ u_1\rangle & \ldots & \langle k,\ u_n\rangle \\ \langle u_1,\ k\rangle & \langle u_1,\ u_1\rangle & \ldots & \langle u_1,\ u_n\rangle \\ \vdots & \vdots & \ddots & \vdots \\ \langle u_n,\ k\rangle & \langle u_n,\ u_1\rangle & \ldots & \langle u_n,\ u_n\rangle \end{vmatrix}.$$

Theorem 3 *Suppose* $x \in L^2[0,\ 1]$, $x : [0,\ 1] \to \mathbb{R}$, *and* $\hat{f} = span\left\{\lambda_{1,\ 0}(t),\ \lambda_{1,\ 1}(t),\ \ldots,\ \lambda_{2^{d-1},\ N-1}(t)\right\}$. *If* $C^T\lambda(t)$ *is the best approximation of x out of* $\hat{f}$, *and we use (7) for approximation of integration x, then the error bound is given by [27]:*

$$\left\|\int_0^t x(s)\,ds - C^T A\lambda(t)\right\|_2 \leq G_x + \Phi_x,$$

where

$$\Phi_x = \frac{\pi_1}{2^{d-1}N}\sum_{n=1}^{2^{d-1}}\left|C_{n,\ N-1}\right|, \quad \text{with } \pi_1 = \max_{t\in[0,\ 1]}\left|\lambda_{n,\ N-1}\right|,\ n = 1,\ \ldots,\ 2^{d-1}.$$

Theorem 4 *Let* $L^2[0,\ 1]$ *be the Hilbert space generated by the Fibonacci wavelet basis. Let* $V(t)$ *be the continuous bounded function in* $L^2[0,\ 1]$. *Then, the Fibonacci wavelet expansion of* $V(t)$ *converges to it.*

$$V(t) = \sum_{i=1}^{2^{\frac{d-1}{2}}}\sum_{j=0}^{N-1} d_{i,\ j}\lambda_{i,\ j}(t),$$

where $d_{i,\ j} = \langle V(t),\ \lambda_{i,\ j}(t)\rangle$. Thus,

$$d_{i,\ j} = \int_0^1 V\left(\frac{\rho + n - 1}{2^{d-1}}\right)\frac{2^{(d-1)/2}}{\sqrt{\Phi_n}}F_n\left(2^{d-1}t - n + 1\right) \times \lambda_{i,\ j}(t)\,dt, \quad \frac{n-1}{2^{d-1}} \leq t \leq \frac{n}{2^{d-1}}.$$

Putting $2^{d-1}t - n + 1 = \rho$ then,

$$d_{i,\ j} = \frac{2^{-(d-1)/2}}{\sqrt{\Phi_n}}\int_0^1 V\left(\frac{\rho - 1 + n}{2^{d-1}}\right)F_n(\rho)\,d\rho.$$

Using the mean value theorem for integration, we have:

$$d_{i,\,j} = \frac{2^{-(d-1)/2}}{\sqrt{\Phi_n}} V\left(\frac{\sigma - 1 + n}{2^{d-1}}\right) \times \int_0^1 F_n\left(\rho\right) d\rho,$$

where $\sigma \in (0,\ 1)$ and choose $\int_0^1 F_n\left(\rho\right) d\rho = \zeta$, then

$$d_{i,\,j} = \frac{2^{-(d-1)/2}}{\sqrt{\Phi_n}} \zeta V\left(\frac{\sigma - 1 + n}{2^{d-1}}\right),\ \ \forall \sigma \in (0,\ 1)\,.$$

Therefore,

$$\left|d_{i,\,j}\right| = \left|\zeta \frac{2^{-(d-1)/2}}{\sqrt{\Phi_n}}\right| \left|V\left(\frac{\sigma - 1 + n}{2^{d-1}}\right)\right|.$$

Since V is bounded by M,

$$\left|d_{i,\,j}\right| \leq \left|\zeta \frac{2^{-(d-1)/2}}{\sqrt{\Phi_n}}\right| M.$$

As the series $\sum_{h=1}^{\infty} \sum_{k=0}^{\infty} d_{i,\,j}$ is absolutely convergent, it follows that the series expansion of $V\left(t\right)$ converges uniformly.

4 Application

We numerically approximated the dynamics of a modified mass balance-surface energy balance model of cryosphere (3) by using the proposed Fibonacci wavelet collocation approach for the following parameters. The time interval is $0 : 0.001 : 1$. A small step size gives high

Table 1. Parameters and their definitions, values and related source

Parameter	Definition	Value	Source
α	A parameter that influences the rate of change of the temperature difference.	1.01	[8]
β	A coefficient representing the interaction between sea-ice extent and temperature variations.	0.1	[8]
γ	Representing the effect of seasonal solar forcing.	1.4	[8]
δ	Frequency of the periodic solar forcing.	0.9	[8]
R	The radiative forcing of CO_2 gas, incorporated to analyze the effects of global warming on the cryosphere system.	0, 1.66, 1.89	[8]
$\wp$	The fractional order of the system.	$0 < \alpha < 1$	Assumed
$s\left(t\right)$	Sea-ice extent.		[8]
$\eta\left(t\right)$	The difference between ocean surface temperature and sea-ice extent.		[8]

numerical precision and prevents instability in the fractional-order system. For these parameter values, the system (2) has three equilibrium points calculated in [8]. The equilibrium points are calculated at $t = 0$ given by: $E_1 = (-0.606097 + 1.00103i,\ 0)$, $E_2 = (1.21219,\ 0,)$, and $E_3 = (-0.606097 - 1.00103i,\ 0)$. They showed that the system (2) is asymptotically stable at all three equilibrium points. The authors of [8] used the parameter $R = 0,\ 1.66,\ 1.89$ to represent external influences such as greenhouse gas forcing. The primary goal of this study is to use

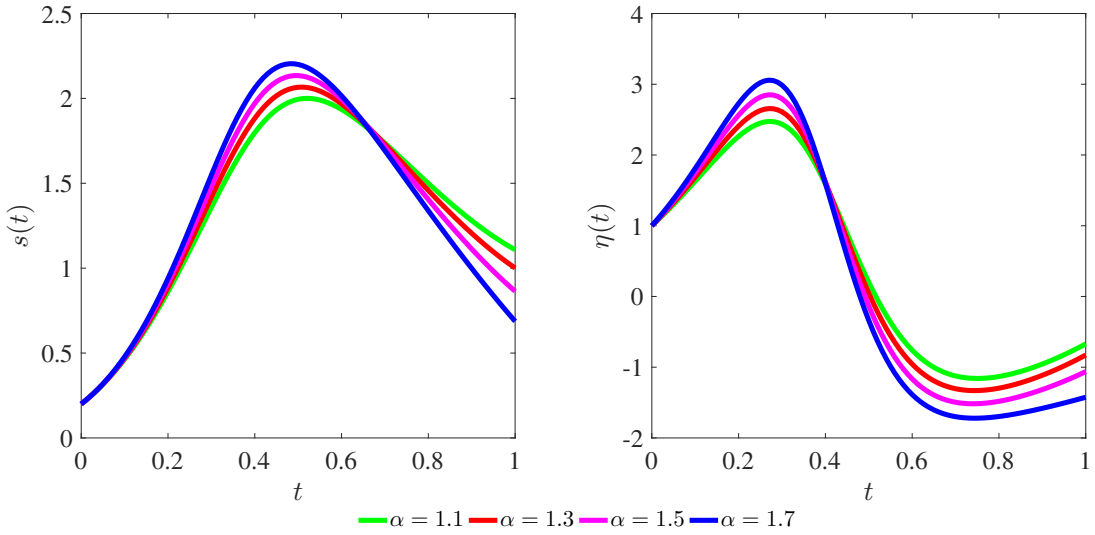

Figure 1. Solution of system (3) for $s\,(0) = 0.2$, $\eta\,(0) = 1$, $\wp = 0.85,\ \beta = 0.1$, $\gamma = 1.4$, $\delta = 0.9,\ R = 1.66$

the fast FW and collocation approach to solve the fractional cryosphere system (3). We solved the fractional cryosphere model in the C-F derivative operator numerically using the fast FW collocation approach described in Section 3. We also compared the results obtained with those of the fourth-order and seventh-order fractional Runge-Kutta (RK4 and RK7, respectively) methods. Our theoretical approaches are validated by the following graphical findings. Figure 1 illustrates the numerical results of the proposed system for different values of α, Figure 2 for different values of $\wp$ and Figure 3 for different values of β. A small changes in the fractional order value $\wp$ and parameters α, β significantly affect the model results. The following figures show that the cryosphere system exhibits oscillatory behavior in our fractional system (3) for the given set of parameters. In all figures of the cryosphere system, the effects of varying the fractional order $\wp$ and other model parameters on each state variable are more clearly seen. For the starting conditions $s\,(0) = 1$ and $\eta\,(0) = 2$, we display the approximation of the system (3) in Figure 4. The findings demonstrate that the oscillating behaviors of the system solution increase when $\wp$ decreases from 0.60 to 0.50. Numerical simulations were performed with $s\,(0) = 2$, $\eta\,(0) = 4$, $\alpha = 1.01$, $\beta = 0.1$, $\gamma = 1.4$, $\delta = 0.9$, and $R = 0$ are represented by numerical simulations. Figure 5 (a) - (d) show that the system solutions oscillate very fast when $\wp$ decreases from 0.65 to 0.45, which is one of the causes of chaos and instability in the system. The results show that a small change in the fractional order significantly impacts the behavior of the model. Specifically, as $\wp$ decreases, the system exhibits more oscillatory behavior, indicating increased sensitivity to fractional-order variations. Table 2 and Table 3 present a comparison of the proposed model solutions using the fast Fibonacci wavelet collocation method and the fractional fourth-order Runge-Kutta method for the parameter values $s\,(0) = 1$, $\eta\,(0) = 2$ and $\wp = 0.90$ & $0.85,\ \alpha = 1.01,\ \beta = 0.1,\ \gamma = 1.33,\ \delta = 0.9,\ R = 1.66$. This comparison demonstrates that the two numerical approaches provide excellent agreement

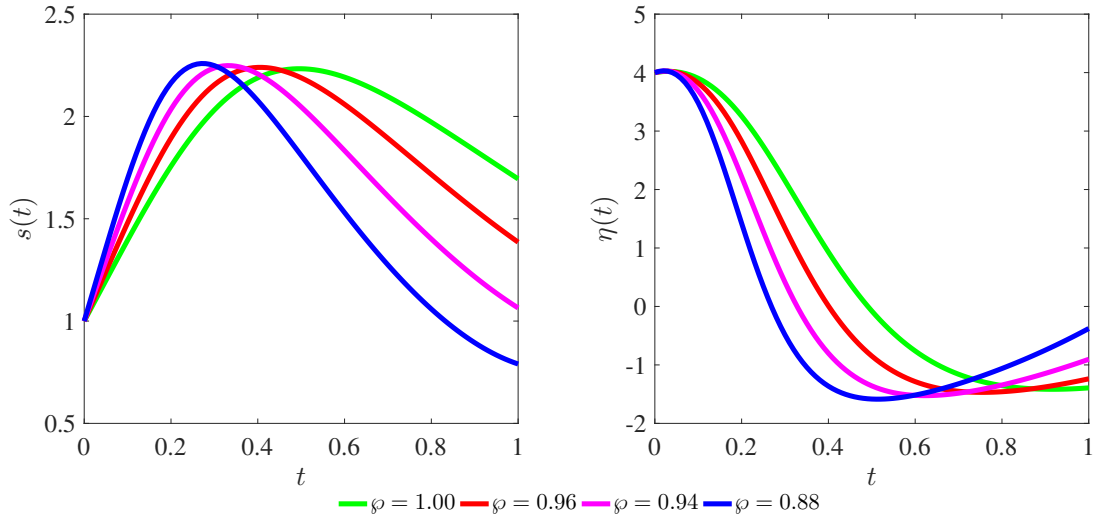

Figure 2. Solution of system (3) for $s\,(0) = 1, \eta\,(0) = 4, \alpha = 1.01, \beta = 0.1, \gamma = 1.4, \delta = 0.9,\ R = 1.66$

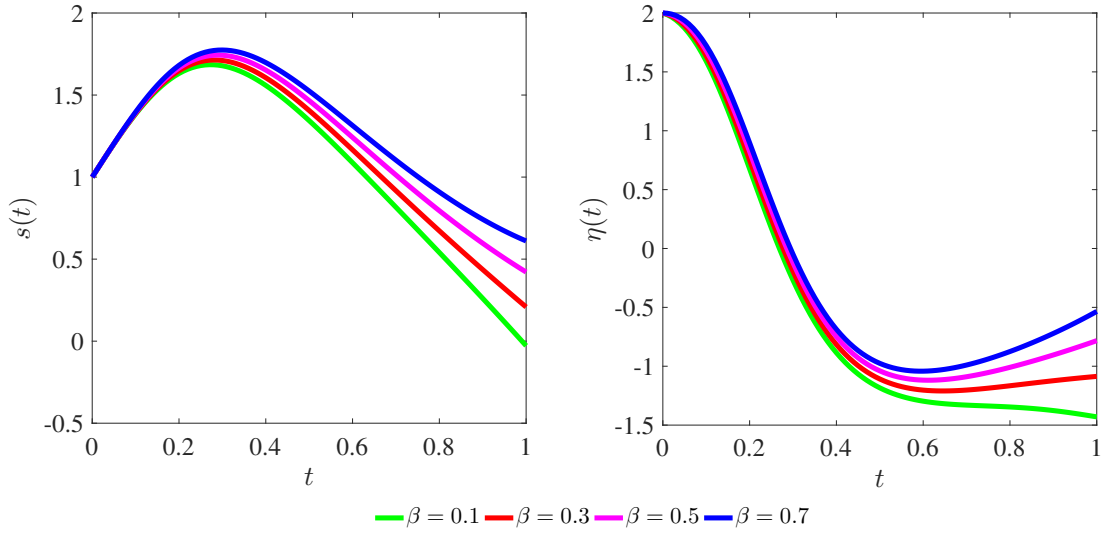

Figure 3. Solution of system (3) for $s\,(0) = 1, \eta\,(0) = 2, \wp = 0.85,\ \alpha = 1.01, \gamma = 1.4, \delta = 0.9,\ R = 0$

in approximating the proposed fractional system of differential equations. The inclusion of the parameter $R = 1.66,\ 1.89$ has its own impact on the approximate results of the given system. In Figure 6 (a)-(d), as we change the values of $\wp$ from $\wp = 0.65$ to $\wp = 0.55,\ 0.50,\ 0.40$, the nature of system (3) shows more oscillatory. Figure 7 is plotted for the parameter $R = 1.89$. For the fractional-order $\wp = 0.5$, Figure 8 and $\wp = 0.98$, Figure 9 present comparison between the fast FW collocation method and the seventh-order Runge-Kutta method (RK7) to approximate the results for system (3). As shown in the graphical illustration, the solutions of the present method align closely with those of the RK7 technique. The graphical results show excellent agreement between the two methods, validating the accuracy and reliability of the FW approach. For fractional orders $\wp = 0.45$ and $\wp = 0.60$, the model results depicted in Figure 10 confirm this agreement.

Table 4 and Table 5 show the comparison of fast FW solutions and the seventh-order Runge-Kutta fractional method (RK7) for the parameter values $s\,(0) = 2, \eta\,(0) = 4$ and $\wp = 0.65\ \&\ 0.50,\ \alpha = 1.01, \beta = 0.1, \gamma = 1.33, \delta = 0.9,\ R = 1.66$. This comparison confirms that the two approximations provide a nice agreement for the proposed system of fractional differential equations. In summary,

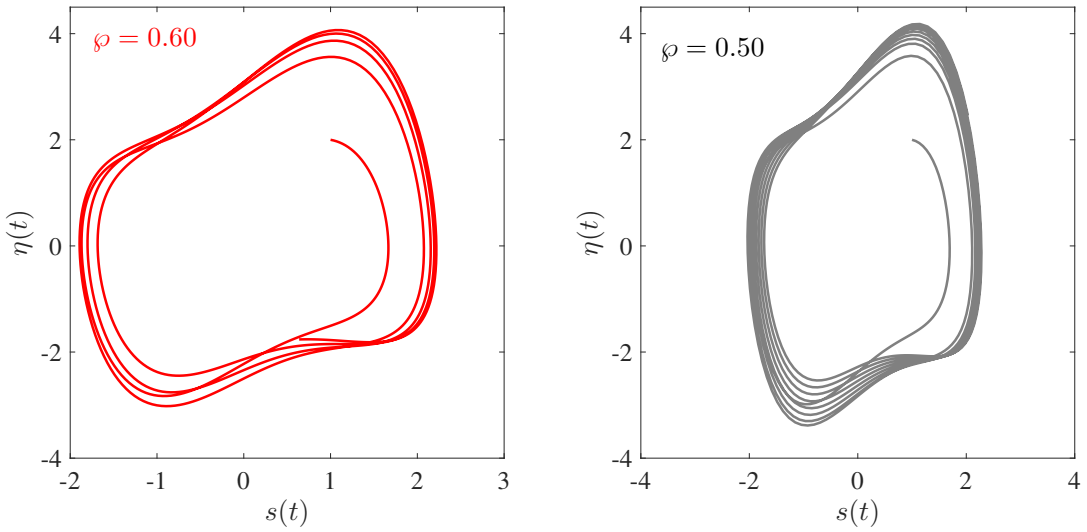

Figure 4. Behavior of the system (3) for $s\,(0) = 1, \eta\,(0) = 2, \alpha = 1.01, \beta = 0.1, \gamma = 1.4, \delta = 0.9,\ R = 0$

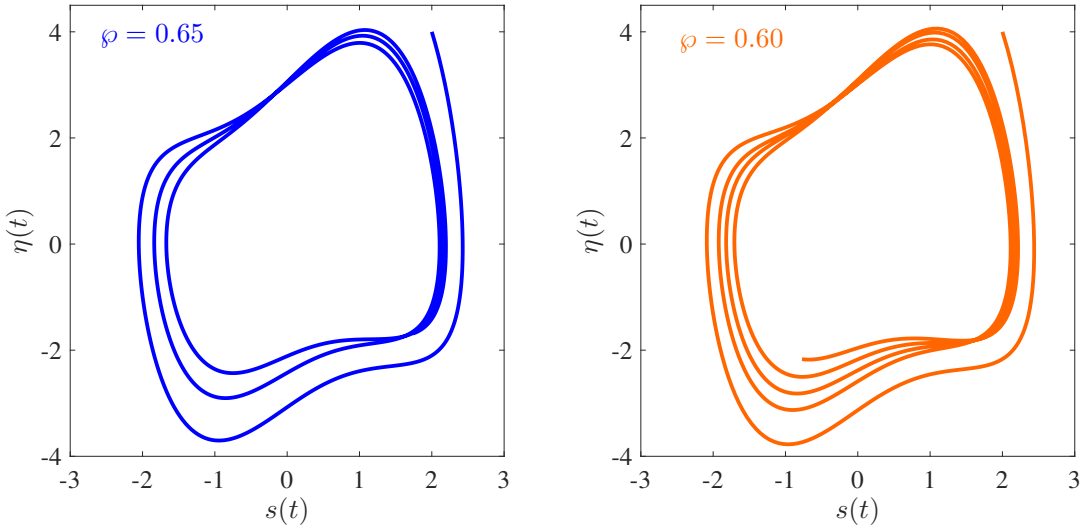

the accuracy of the proposed scheme was verified by comparing the results with the RK4 and RK7 schemes.

5 Conclusion

The mathematical models related to climate have attracted significant attention from meteorologists and mathematicians in recent years. In this study, the C-F fractional derivative operator with a non-singular exponential decay kernel was used to represent the cryosphere model. This system was successfully solved using the FW and collocation approaches. The graphical and tabular results highlight the accuracy of the fast Fibonacci wavelet collocation method in solving the fractional cryosphere model. The fractional order $\wp$ plays a crucial role in determining the system's behavior. Lower values of $\wp$ lead to more oscillatory and potentially chaotic dynamics. This sensitivity underscores the importance of accurately selecting $\wp$ in fractional modeling. The cryosphere model exhibits significant oscillatory behavior, especially at lower fractional orders.

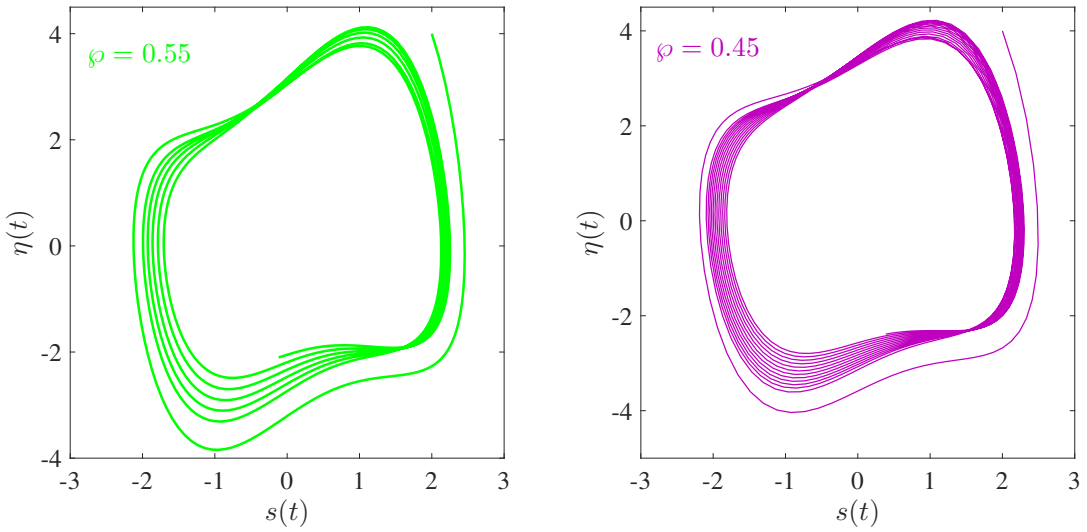

Figure 5. Behavior of the system (3) for $s\,(0) = 2, \eta\,(0) = 4, \alpha = 1.01, \beta = 0.1, \gamma = 1.4, \delta = 0.9,\ R = 0$

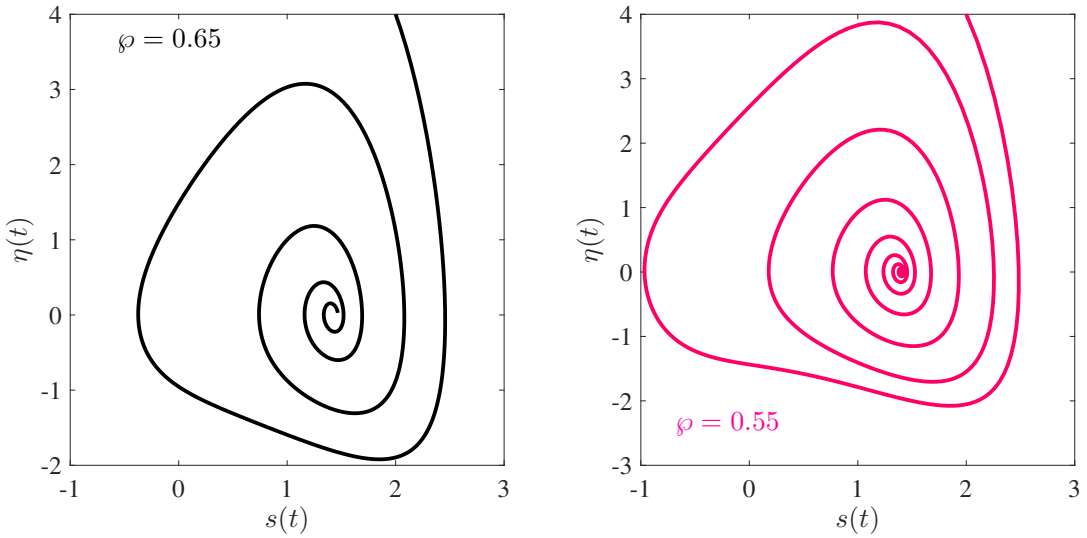

This oscillatory nature can be attributed to the nonlinear interactions within the system, which are more pronounced under fractional dynamics. The close agreement between the FW method and the RK4 and RK7 methods validates the accuracy and reliability of the FW approach. The FW method's computational efficiency is evident from its ability to handle complex fractional differential equations with relatively low computational cost. This efficiency, combined with its accuracy, makes the FW method a viable alternative to traditional numerical methods like RK4 and RK7. The numerical results highlight the strength and efficiency of this method in predicting solutions for various fractional dynamical systems. The method's low computational cost and ease of implementation further enhance its applicability to various models. The graphical view of arbitrary-order cryosphere model equations was obtained using MATLAB R2016a mathematical software. We made a comparison of the proposed numerical scheme with the fractional order Runge-Kutta methods of fourth and seventh orders, and we confirmed all techniques are in good agreement to approximate the dynamical system of fractional differential equations. Future

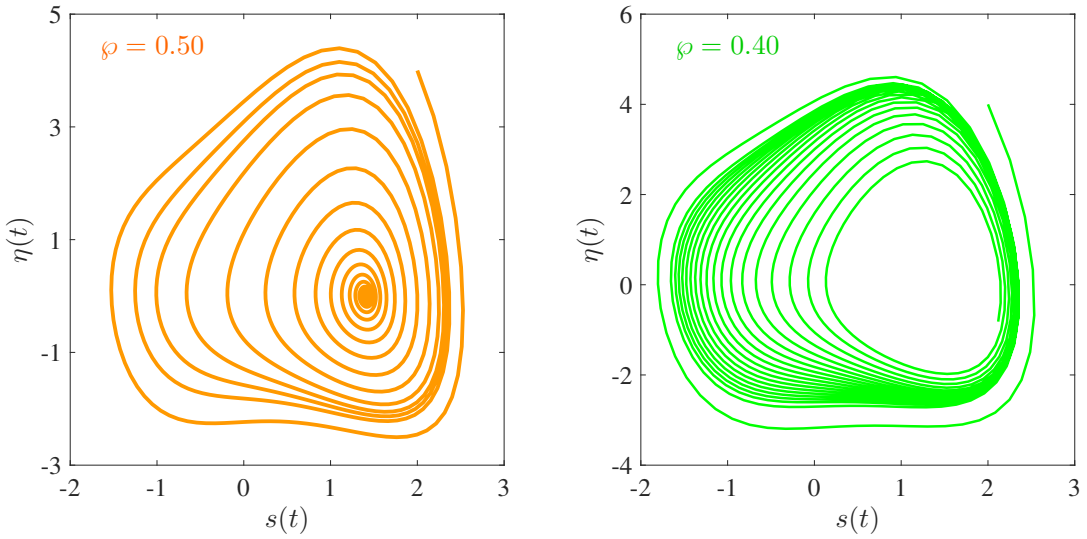

Figure 6. Behavior of the system (3) for $s\,(0) = 2, \eta\,(0) = 4, \alpha = 1.01, \beta = 0.1, \gamma = 1.4, \delta = 0.9,\ R = 1.66$

Table 2. Comparison of the fast Fibonacci wavelet with fractional RK4 method for $s\,(t)$

$\wp$	t	$s\,(t)$ (Fibonacci wavelet method)	$s\,(t)$ (RK4 method)
	0.0	1.000000000000	1.000000000000
	0.1	1.40920844794	1.40931361776
0.90	0.3	1.81880108549	1.81564846875
	0.5	1.61254460793	1.60949913423
	0.7	1.28319151944	1.28275766929
	0.9	1.09543423589	1.0978666704
	0.0	2.000000000000	2.000000000000
	0.1	1.56233863163	1.56179166173
0.85	0.3	1.71221314383	1.70716793396
	0.5	1.22228387678	1.22200234476
	0.7	1.00065799683	1.00607782481
	0.9	1.27143424615	1.27655837342

Table 3. Comparison of the fast Fibonacci wavelet with fractional RK4 method for $\eta\,(t)$

$\wp$	t	$\eta\,(t)$ (Fibonacci wavelet method)	$\eta\,(t)$ (RK4 method)
	0.1	1.83147856293	1.82329768002
0.90	0.3	0.0522728475454	0.0461506843707
	0.5	-0.810174033811	-0.813766161049
	0.7	-0.684875546167	-0.686215510625
	0.9	-0.180912606179	-0.184164235964
	0.1	1.53073311857	1.53486488777
0.85	0.3	-0.70171625209	-0.706655755863
	0.5	-0.719672443074	-0.717183987406
	0.7	0.0446686806895	0.0422412317858
	0.9	0.745305737021	0.741110005206

research will focus on modification of this model by incorporating additional parameters to investigate their effects on climate change and applying recent fractional operators with new numerical approaches, as it is still open. The FW method's adaptability and efficiency make it a promising tool for future investigations in climate modeling and other fields involving fractional differential

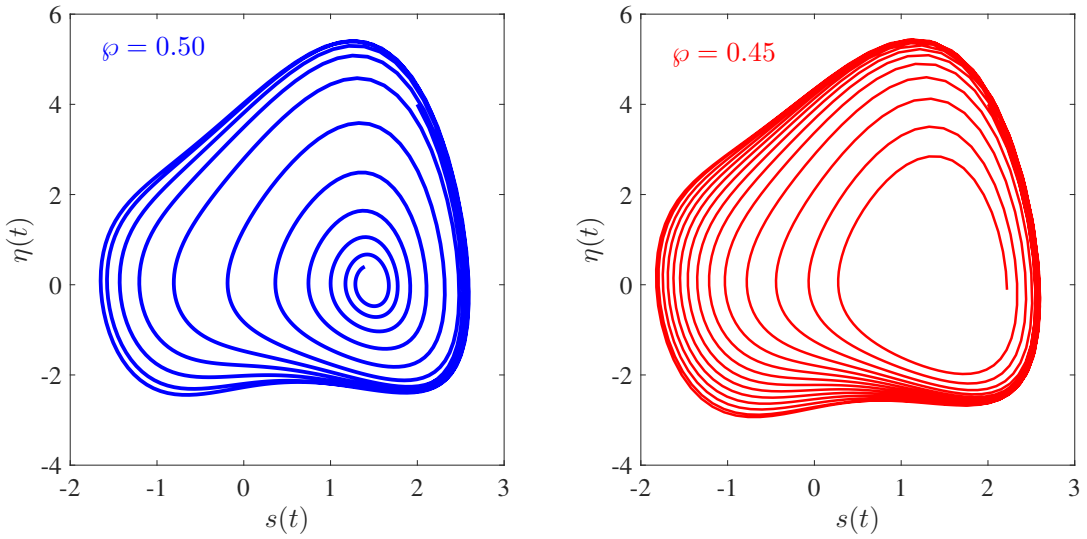

Figure 7. Behavior of the system (3) for $s\,(0) = 2$, $\eta\,(0) = 4$, $\alpha = 1.3$, $\beta = 0.1$, $\gamma = 1.4$, $\delta = 0.9$, $R = 1.89$

Table 4. Comparison of the fast Fibonacci wavelet method $(d = 1,\ N = 10)$ with RK7 method

$\wp$	t	$s\,(t)$ (Fibonacci wavelet method)	$s\,(t)$ (RK7 method [8])
	0.2	-0.371446547494	-0.253573572216
0.65	0.4	1.29377789648	1.17845168413
	0.6	1.62488732726	1.50717658469
	0.8	1.5184545495	1.64905771613
	0.2	-0.44162568796	-0.809978922532
0.50	0.4	1.15579349906	1.37164633506
	0.6	1.3433829426	1.35303777093
	0.8	1.40981168304	1.38632479674

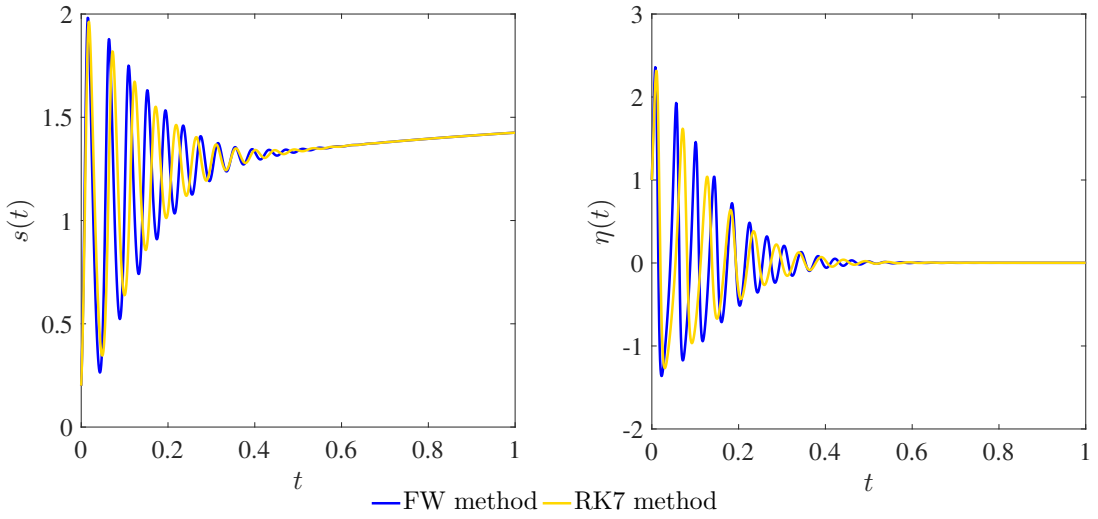

Figure 8. Numerical results of (3) for $\wp = 0.5$, $\alpha = 1.01$, $\beta = 0.1$, $\gamma = 1.4$, $\delta = 0.9$, $R = 1.66$

equations. In conclusion, the fast Fibonacci wavelet collocation method proves to be a robust and efficient numerical approach for solving the fractional cryosphere model. The method's ability to accurately capture the system's dynamics, coupled with its computational efficiency, makes

Table 5. Comparison of the fast Fibonacci wavelet method $(d = 1,\ N = 10)$ with RK7 method

$\wp$	t	$\eta\,(t)$ (Fibonacci wavelet method)	$\eta\,(t)$ (RK7 method [8])
0.65	0.2	-0.286738763533	-0.239539900977
	0.4	-1.002037886	-0.965385123168
	0.6	-0.485697132823	-0.480615290519
	0.8	-0.00876895053594	-0.00838931451505
0.50	0.2	0.697013352679	0.697013352679
	0.4	1.33907761927	1.33907135154
	0.6	-0.299945151616	-0.29838119306
	0.8	0.0464768418089	0.0469004528939

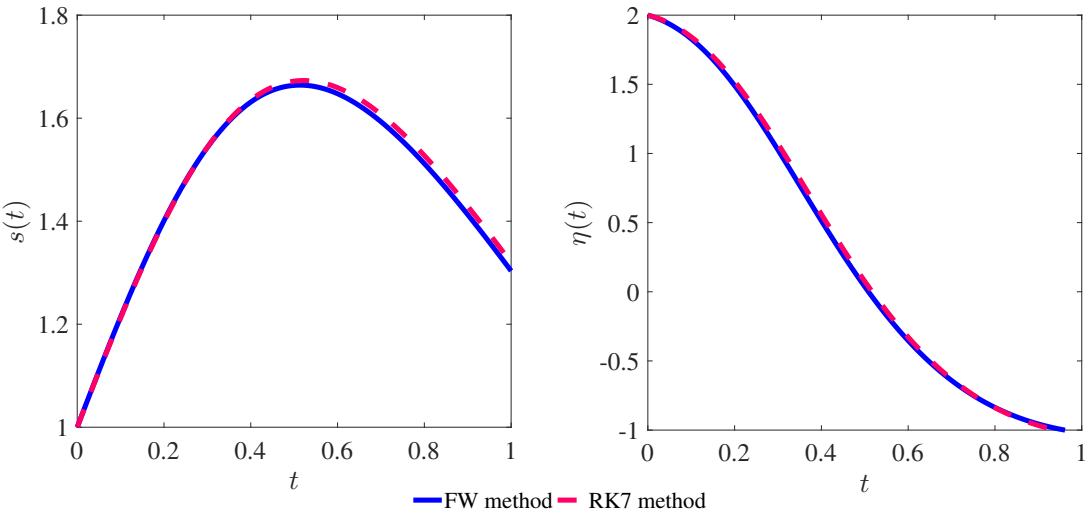

Figure 9. Numerical results of (3) for $\wp = 0.98,\ \alpha = 1.01,\ \beta = 0.1,\ \gamma = 1.33,\ \delta = 0.9,\ R = 0$

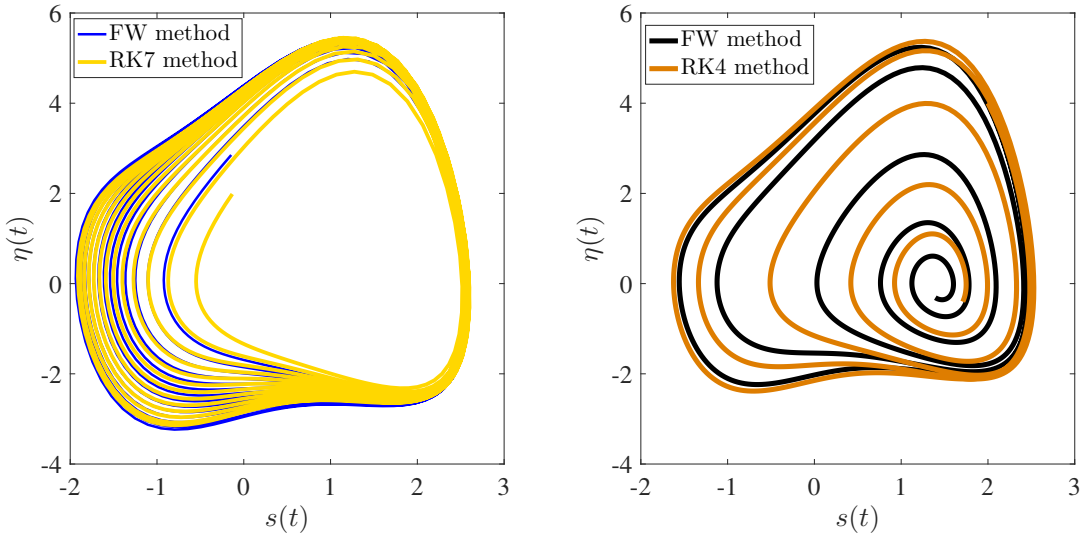

Figure 10. Comparison of Fibonacci wavelet method with a. RK7 method $(\wp = 0.45)$, b. RK4 method $(\wp = 0.6)$ for $s_0 = 2,\ \eta_0 = 4,\ \alpha = 1.3,\ \beta = 0.1,\ \gamma = 1.4,\ \delta = 0.9,\ R = 1.66$

it a valuable tool for researchers and practitioners in the field of fractional calculus and climate modeling.

Declarations

Use of AI tools

The author declares that he has not used Artificial Intelligence (AI) tools in the creation of this article.

Data availability statement

No data are associated with this manuscript.

Ethical approval (optional)

The author states that this research complies with ethical standards. This research does not involve either human participants or animals.

Consent for publication

Not applicable

Conflicts of interest

The author declares no conflicts of interest.

Funding

No funding was received for this research.

Author's contributions

The author has written, read, and agreed to the published version of the manuscript.

Acknowledgements

Not applicable

References

[1] Aychluh, M. Nonlinear analysis of the fractional Lorenz-84 model with a Rabotnov exponential kernel law. *Journal of Applied Mathematics and Computing*, 71(2), 2231-2260, (2025). [CrossRef]

[2] Marshall, S.J. *The Cryosphere*. Princeton University Press: New Jersey, (2011).

[3] Deng, K., Azorin-Molina, C., Yang, S., Hu, C., Zhang, G., Minola, L. and Chen, D. Changes of Southern Hemisphere westerlies in the future warming climate. *Atmospheric Research*, 270, 106040, (2022). [CrossRef]

[4] Habenom, H., Aychluh, M., Suthar, D.L., Al-Mdallal, Q. and Purohit, S.D. Modeling and analysis on the transmission of covid-19 Pandemic in Ethiopia. *Alexandria Engineering Journal*, 61(7), 5323-5342, (2022). [CrossRef]

[5] Aychluh, M., Purohit, S.D., Agarwal, P. and Suthar, D.L. Atangana–Baleanu derivative-based fractional model of COVID-19 dynamics in Ethiopia. *Applied Mathematics in Science and Engineering*, 30(1), 635-660, (2022). [CrossRef]

[6] Diethelm, K. *The Analysis of Fractional Differential Equations: An Application-Oriented Exposition Using Differential Operators of Caputo Type* (Vol. 2004). Springer: Berlin, (2010). [CrossRef]

[7] Caputo, M. and Fabrizio, M. A new definition of fractional derivative without singular kernel. *Progress in Fractional Differentiation & Applications*, 1(2), 73-85, (2015). [CrossRef]

[8] Chakraborty, A., Veeresha, P., Ciancio, A., Baskonus, H.M. and Alsulami, M. The effect of climate change on the dynamics of a modified surface energy balance-mass balance model of Cryosphere under the frame of a non-local operator. *Results in Physics*, 54, 107031, (2023). [CrossRef]

[9] Nicolis, C. Long-term climatic transitions and stochastic resonance. *Journal of Statistical Physics*, 70, 3–14, (1993). [CrossRef]

[10] Aychluh, M., Suthar, D.L. and Purohit, S.D. Analysis of the nonlinear Fitzhugh–Nagumo equation and its derivative based on the Rabotnov fractional exponential function. *Partial Differential Equations in Applied Mathematics*, 11, 100764, (2024).[CrossRef]

[11] Aychluh, M. and Ayalew, M. The fractional power series method for solving the nonlinear Kuramoto-Sivashinsky equation. *International Journal of Applied and Computational Mathematics*, 11, 29, (2025). [CrossRef]

[12] Keshavarz, E., Ordokhani, Y. and Razzaghi, M. Bernoulli wavelet operational matrix of fractional order integration and its applications in solving the fractional order differential equations. *Applied Mathematical Modelling*, 38(24), 6038-6051, (2014). [CrossRef]

[13] Ayalew, M., Ayalew, M. and Aychluh, M. Numerical approximation of space-fractional diffusion equation using Laguerre spectral collocation method. *International Journal of Mathematics for Industry*, 1-17, (2024). [CrossRef]

[14] Heydari, M.H., Hooshmandasl, M.R. and Ghaini, F.M. A new approach of the Chebyshev wavelets method for partial differential equations with boundary conditions of the telegraph type. *Applied Mathematical Modelling*, 38(5-6), 1597-1606, (2014).[CrossRef]

[15] Suthar, D.L., Habenom, H. and Aychluh, M. Effect of vaccination on the transmission dynamics of COVID-19 in Ethiopia. *Results in Physics*, 32, 105022, (2022). [CrossRef]

[16] Ur Rehman, M. and Saeed, U. Gegenbauer wavelets operational matrix method for fractional differential equations. *Journal of the Korean Mathematical Society*, 52(5), 1069-1096, (2015). [CrossRef]

[17] Iqbal, M.A., Saeed, U. and Mohyud-Din, S.T. Modified Laguerre wavelets method for delay differential equations of fractional-order. *Egyptian Journal of Basic and Applied Sciences*, 2(1), 50-54, (2015). [CrossRef]

[18] Venkatesh, S.G., Ayyaswamy, S.K. and Balachandar, S.R. Legendre Wavelets based approximation method for solving advection problems. *Ain Shams Engineering Journal*, 4(4), 925-932, (2013). [CrossRef]

[19] Srinivasa, K. and Mundewadi, R.A. Wavelets approach for the solution of nonlinear variable delay differential equations. *International Journal of Mathematics and Computer in Engineering*, 1(2), 139-148, (2023). [CrossRef]

[20] Mulimani, M. and Srinivasa, K. A new approach to the Benjamin-Bona-Mahony equation via ultraspherical wavelets collocation method. *International Journal of Mathematics and Computer in Engineering*, 2(2), 179-192, (2024). [CrossRef]

[21] Golberg, M. and Chen, C. *Discrete Projection Methods for Integral Equations*. Computational Mechanics: Boston, (1996). [CrossRef]

[22] Shiralashetti, S.C. and Lamani, L. Fibonacci wavelet based numerical method for the solution of nonlinear Stratonovich Volterra integral equations. *Scientific African*, 10, e00594, (2020).

[23] Sabermahani, S., Ordokhani, Y. and Yousefi, S.A. Fibonacci wavelets and their applications for solving two classes of time-varying delay problems. *Optimal Control Applications and Methods*, 41(2), 395–416, (2020). [CrossRef]

[24] Sabermahani, S. and Ordokhani, Y. Fibonacci wavelets and Galerkin method to investigate fractional optimal control problems with bibliometric analysis. *Journal of Vibration and Control*, 27(15-16), 1778-1792, (2021). [CrossRef]

[25] Srivastava, H.M., Shah, F.A. and Nayied, N.A. Fibonacci wavelet method for the solution of the non-linear Hunter–Saxton equation. *Applied Sciences*, 12(15), 7738, (2022). [CrossRef]

[26] Shah, F.A., Irfan, M., Nisar, K.S., Matoog, R.T. and Mahmoud, E.E. Fibonacci wavelet method for solving time-fractional telegraph equations with Dirichlet boundary conditions. *Results in Physics*, 24, 104123, (2021). [CrossRef]

[27] Vivek, Kumar, M. and Mishra, S.N. A fast Fibonacci wavelet-based numerical algorithm for the solution of HIV-infected $CD4^+$ T cells model. *The European Physical Journal Plus*, 138, 458, (2023). [CrossRef]

[28] Chakraborty, A. and Veeresha, P. Effects of global warming, time delay and chaos control on the dynamics of a chaotic atmospheric propagation model within the frame of Caputo fractional operator. *Communications in Nonlinear Science and Numerical Simulation*, 128, 107657 (2024). [CrossRef]

[29] Kumbinarasaiah, S. and Mulimani, M. Fibonacci wavelets-based numerical method for solving fractional order (1+1)-dimensional dispersive partial differential equation. *International Journal of Dynamics and Control*, 11, 2232–2255, (2023). [CrossRef]

[30] Moore, E.J., Sirisubtawee, S. and Koonprasert, S. A Caputo–Fabrizio fractional differential equation model for HIV/AIDS with treatment compartment. *Advances in Difference Equations*, 2019(200), 1-20, (2019). [CrossRef]

[31] Losada, J. and Nieto, J.J. Properties of a new fractional derivative without singular kernel. *Progress in Fractional Differentiation and Applications*, 1(2), 87–92, (2015). [CrossRef]

[32] Kumbinarasaiah, S. Hermite wavelets approach for the multi-term fractional differential equations. *Journal of Interdisciplinary Mathematics*, 24(5), 1241-1262, (2021). [CrossRef]

Mathematical Modelling and Numerical Simulation with Applications (MMNSA)
(https://dergipark.org.tr/en/pub/mmnsa)

How to cite this article: Aychluh, M. (2025). Application of a fast Fibonacci wavelet method for the fractional cryosphere model. *Mathematical Modelling and Numerical Simulation with Applications*, 5(2), 257-279. https://doi.org/10.53391/mmnsa.1529457